symmetry

MDPI

Article

On the Application of the Method of Linear Integral Representations to the Local Reconstruction of the Wave Potential

Inna Stepanova [1,*], Alexey Shchepetilov [2], Igor Kolotov [2] and Andrei Levashov [2]

[1] Schmidt Institute of Physics of the Earth, Russian Academy of Sciences, 123995 Moscow, Russia
[2] Department of Physics, Lomonosov Moscow State University, 119991 Moscow, Russia; a_v_shchepetilov@physics.msu.ru (A.S.); corners@list.ru (I.K.); levashov1111@gmail.com (A.L.)
* Correspondence: tet@ifz.ru

Abstract

A new version of the linear integral representation method is developed for solving inverse problems in geophysics. This approach is applied to the interpretation of anomalous time-dependent field data. The reconstruction of field elements is reduced to solving a system of linear algebraic equations (SLAE) with an approximately given right-hand side. Since the matrix elements of this system are derived analytically, the modeling process is significantly simplified. The article also analyzes how the approximation quality of a non-stationary field element depends on the observation network geometry, enabling its optimization for more accurate detection of geological properties. The proposed method for solving inverse problems for hyperbolic partial differential equations with constant coefficients can also be applied to data described by systems of nonlinear PDEs, provided the target field is represented as a composition of components differing in magnitude. Finally, the results of non-stationary gravity field modeling are presented.

Keywords: gravity field; non-stationary field; Green function; linear integral representations

1. Introduction

Nowadays, processing large and ultra-large datasets of Earth and solar system physical fields has become routine. While the high resolution and reliability of satellite data represent a pinnacle of science and technology, this abundance of information can create an illusion that once "impenetrable" interpretation problems are now easily solvable. Nevertheless, the sources of both stationary and, especially, non-stationary fields cannot be uniquely reconstructed from any amount of data without a priori information regarding their geometry and depth. Unprecedented detail in imaging planetary surfaces does not inherently guarantee progress in solving inverse problems of mathematical physics and geophysics, which require identifying field sources or the underlying causes of physical phenomena. The method of linear integral representations in its classical form preserves the continuous nature of a medium while utilizing a finite, often limited, dataset.

Backus and Gilbert [1–3] proposed an effective approach for geophysical problems requiring pointwise reconstruction of field sources (1D) or spatial distributions (3D). This method is widely used in seismic tomography, where images inferred from seismic data constrain models of the Earth's internal structure, composition, and dynamics [4]. Although popular finite-parameter models are also employed within this framework, they impose stringent conditions on the kernels of the integral equations. These kernels are highly

Check for updates

Received: 6 February 2026
Revised: 16 March 2026
Accepted: 20 March 2026
Published: 23 March 2026

Copyright: © 2026 by the authors. Licensee MDPI, Basel, Switzerland. This article is an open access article distributed under the terms and conditions of the Creative Commons Attribution (CC BY) license.

sensitive to projection onto finite-dimensional subspaces and must be computed accurately to reflect the real properties of the geological environment.

Finite-frequency models are typically implemented in two steps: (1) introducing a model space with a finite number of parameters (which may inadequately represent geological objects) and (2) applying damped least-squares (DLS) methods to evaluate these parameters. As Backus and Gilbert noted [1], the collection of Earth models yielding physically observed values for any independent dataset is "either empty or infinite-dimensional." The linear Backus–Gilbert algorithm aims to restore unbiased, spatially distributed averaged properties. In essence, the method determines unknown linear functionals of a target function based on a finite number of known linear functionals. Typically, these are represented as integrals over a manifold with a given measure. A constrained variational problem is then formulated and reduced to an unconstrained one using Lagrange multipliers. The resulting vector of multipliers is determined by solving a system of linear algebraic equations (SLAE), which is usually symmetric and positive semidefinite.

Since most tomographic problems are underdetermined, solving them within this framework necessitates efficient regularization algorithms. In [5], an original technique was developed to determine tomographic images using the classical Backus–Gilbert method without relying on finite-frequency approximations. Beyond geophysics, this method is crucial in spectroscopy, where obtaining spectral densities from lattice data is vital for quantum field theory [6,7].

The transition to a system of linear algebraic equations raises a key question: what properties must the matrix possess—and how must it depend on the observation network geometry—to ensure that solutions are robust against noise? Ideally, one should avoid excessive distortion of the forward problem operator to remain close to the continuous medium model. However, a fundamental shift in interpretation theory—across geophysical, biophysical, and astrophysical data—is the transition toward discrete field theories. In this context, integral representations allow for the efficient calculation of field values at any point, including boundaries. Since data are often provided on irregular grids with gaps or errors, calculating values on specific point sets enables a constructive solution to the inverse problem, for instance, by using the tridiagonal matrix algorithm (Thomas algorithm).

Our goal is to establish conditions and constraints that yield analytical expressions (in terms of elementary or special functions) for the SLAE matrix elements. This keeps the forward problem operator unperturbed, simplifying the selection or development of regularization algorithms. Notably, the classical Backus–Gilbert method does not require discretization of the integral operator.

The proposed methodology for non-stationary fields may also be applicable to other "self-consistent" fields (gravitational, magnetic, electrical, thermal, etc.). If an unknown signal is decomposed into components of differing magnitudes, some may satisfy simpler equations and boundary conditions, significantly reducing the complexity of the inverse problem. Finally, the possibility of an initially discrete formulation remains a fundamental consideration.

Wave motions occur in various scientific fields, including elastic waves in the Earth's core, gas and fluid dynamics, and electromagnetics. The arsenal for solving direct and inverse problems for the wave operator is extensive [8–16]. If the wave source function $\overline{f}(\overline{x}, t)$ is unknown, the approach developed by Yamamoto [8,9] can be applied, utilizing Lagrange multipliers and Hilbert space methods to establish solution uniqueness. This technique successfully reconstructs point sources in 1D cases, while the reciprocity gap functional method enables the determination of smoothly distributed 3D sources using boundary observations. The Yamamoto approach was further refined in [10–16].

In our previous works [17,18], we demonstrated how the method of linear integral representations and discrete field theory can be applied to linear and nonlinear inverse problems in geophysics. Unlike parameter-based models of geological media, we do not abandon the infinite-dimensional continuum. Instead, we initially treat both the observation space and its defined functions as discrete, imposing no constraints on values between grid nodes. This representation necessitates a reconsideration of the relationships between macro- and micro-levels. Here, the fundamental solution to the Laplace equation is replaced by its discrete analog, which lacks delta-function singularities; instead, a unit impulse exists at a point. Furthermore, unlike the continuous case, the discrete fundamental solution may be non-unique.

The S-approximation method is based on the integral representation of harmonic functions (Green's formula), where anomalous field sources are distributed on one or more planes. We also developed a modified S-approximation method, incorporating specific features of the unknown source into the quality functional. Matrix elements in this method have simple analytical forms, expressed via elementary functions (local version) or elliptic integrals (regional version).

The novelty of our technique lies in the following:

1. Accurate reconstruction of spatial source distributions from a finite set of values of a single anomalous field element.
2. Introduction of new constraints on the upper and lower bounds of the least-mean-square (LMS) misfit.
3. Establishment of the "admissible solution" concept, which is critical for geophysical applications.
4. Reduction in interpretation problems to systems of linear algebraic equations (SLAE) with symmetric, non-negative matrices whose elements are derived analytically.
5. Development of the modified S-approximation, minimizing an additional quality functional over the set of admissible solutions.
6. Regularization of the three-level Chebyshev iterative method for solving SLAEs within the integral representation framework.
7. Development of the block contrasting method (BCM) for large-scale data, partitioning the study area into subdomains of intense anomalies.
8. Demonstrated effectiveness on models with sharp elevation changes and irregular grids across various signal-to-noise ratios.
9. Application of the modified S-approximation to construct linear transforms for interpreting real satellite gravimetric data at a regional scale.

Models of physical fields and topography should evolve smoothly as new information becomes available [19–21]. Radical structural disruptions in a model should be treated with caution; while bifurcation points in nonlinear PDE systems exist, the conditions for such "catastrophes" must be strictly accounted for. Joint inversion of Earth's gravity field variations and topography/bathymetry data—such as from the GRACE mission [22]—remains a priority.

Previously, we did not address inverse problems for hyperbolic PDEs within this framework. This paper discusses a variational setting for determining equivalent sources of a non-stationary field. We formulate the problem for the local case, where the signal satisfies a wave equation with constant coefficients. All a priori information, such as field gradients [23], is incorporated, with time treated as either an independent variable or a parameter [24].

In [25], we applied the global linear integral representation method to the downward continuation of Mercury's magnetic field. Analytical modeling is crucial for solving inverse problems of wave or thermal nature. For reliable source determination, the initial

distribution of field elements and gradients must be defined in 3D space. Assuming the Earth is a half-space, we use Cartesian coordinates, though results can be extended to complex spaces (as with parabolic operators). This article formulates an inverse problem for the 3D wave equation to determine an unknown vector source function of space and time, assuming homogeneous initial conditions. We establish conditions under which SLAE matrix elements can be obtained via elementary functions, which is fundamental for processing vast, irregular, and noisy datasets in geophysics, astrophysics, and other fields. Otherwise, it would be impossible to ensure that the interpretation results accurately reflect reality. Since inverse problems are almost always ill-posed, they require regularization algorithms for their solution. However, as not all ill-posed problems are regularizable, the search for constructive solutions (i.e., those expressed analytically) remains a perennially relevant task.

2. Methods

In this paper, all variational settings are studied in Cartesian coordinates.

Initial distributions of physical field values and their gradients can be obtained using various versions of the S-approximation method [17,18], even when no information regarding the sources is available. The S-approximation method is based on Green's formula for harmonic functions and variational calculus. To solve the linear inverse problem in geophysics, a regularized variational problem is formulated. This method is highly efficient when a priori information about field sources is heterogeneous and approximate, allowing equivalent sources of the external field (gravity or magnetic) to be found with high relative accuracy. While this facilitates the mathematical modeling of stationary geophysical fields, stationary vector fields are far less common than non-stationary ones.

The aim of our research is to develop a fundamentally new approach for solving linear (and subsequently nonlinear) inverse problems for hyperbolic partial differential equations, taking into account the symmetry and other features of the unknown sources. This is particularly relevant when a priori information on the initial and boundary distributions of field elements is scarce or absent. Indeed, geophysical field modeling can be effectively described through direct and inverse settings of this kind.

For example, let us consider the following partial differential equations system [26]:

In this paper, all variational settings are analyzed in Cartesian coordinates. Initial distributions of physical field values and their gradients can be obtained using various versions of the S-approximation method [17,18], even in the absence of source information. Based on Green's formula for harmonic functions and variational calculus, a regularized variational problem is formulated to solve the linear inverse problem. This method is highly efficient when a priori information is heterogeneous or approximate, enabling the reconstruction of equivalent sources for external fields (gravity or magnetic) with high relative accuracy. While this facilitates the modeling of stationary geophysical fields, it should be noted that stationary vector fields are far less common than non-stationary ones.

The aim of our research is to develop a fundamentally new approach for solving linear (and subsequently nonlinear) inverse problems for hyperbolic partial differential equations, accounting for the symmetry and specific features of unknown sources. This is particularly relevant when information on initial and boundary distributions is scarce or unavailable. Indeed, geophysical field modeling can be effectively characterized through such direct

and inverse formulations. For example, let us consider the following system of partial differential equations [26]:

$$\begin{array}{l} \frac{\partial \overline{v}}{\partial t} = -(\overline{v}, \nabla \overline{v}) + \left[\overline{B}, rot\overline{B}\right] - \nabla p, \\ \frac{\partial \overline{B}}{\partial t} = -\left\{\overline{v}, \overline{B}\right\} + \nu \Delta \overline{B}, \\ div\overline{v} = 0,\ div\overline{B} = 0. \end{array} \quad (1)$$

System (1) corresponds to the linearized Euler equations if we consider the motion of a charged fluid within a variational framework. In (1) $\overline{v}(\overline{r}, t)$, $\overline{B}(\overline{r}, t)$ represent the velocity field and magnetic induction, respectively, as functions of spatial coordinates and time; ∇p denotes the pressure gradient in the fluid, and Δ is the Laplace operator. Square brackets denote the cross product of two 3D vectors, while curly brackets relate to the so-called Poisson bracket of two vector fields:

$$\left\{\overline{v}, \overline{B}\right\}_i = \sum_{j=1}^{3} v_j \frac{\partial B_i}{\partial x_j} - B_j \frac{\partial v_i}{\partial x_j}$$

To find an approximate solution to system (1), it is recommended (see [17]) to replace partial differential operators with their finite-difference analogs. Furthermore, initial and boundary conditions imposed on the vector fields $\overline{B}$ and $\overline{v}$ (which are functions of three spatial coordinates and time) must be taken into account. Since magnetic induction and the velocity vector are intrinsically coupled, separating them is a highly complex task. However, a method of successive approximations can be implemented. Specifically, magnetic induction and velocity can be represented as sums of several (finite or infinite) terms of varying magnitudes, allowing us to solve simplified systems similar to (1).

Given a mathematical model for one field, we can formulate a simplified setting for the other. In the general case, such settings involve hyperbolic partial differential operators. To simplify the task, we assume that a portion of the signal satisfies an initial-boundary value problem for a hyperbolic operator with constant coefficients. Various stationary and non-stationary models can be used simultaneously to ensure the maximum efficacy of the approach, provided that heterogeneous and approximate a priori information is available. Even for fields regarded as stationary, we can introduce a parameter that treats all vector fields as non-stationary. Subsequently, the most pertinent solution can be selected based on a priori information that satisfies relative accuracy constraints. If an integral representation holds for a certain component, the other components of the velocity vector or magnetic induction can be found by solving a simpler problem than the original one: they may satisfy a lower-order partial differential equation.

As is well known, the method of descent [24] enables one to find the solution of a boundary value problem in N-dimensional space if the corresponding solution in $(N + 1)$-dimensional space is found. Therefore, a transition from vector functions dependent on three spatial coordinates to those in a four-dimensional space (where the fourth coordinate is time) is considered feasible when constructing metrological approximations of physical field elements and topography.

Let the Earth be represented as the lower half-space bounded by the plane. Let Earth be the lower half-space bounded by the plane $x_3 = 0$ in the Cartesian coordinate system $(x_1\ x_{2,}\ x_3)$.

We can then formulate the Dirichlet boundary value problem for a non-stationary vector field as follows. Let vector functions $\overline{f}(\overline{x}, t) \in C^2\left(\mathbb{R}^3 \times [0, T]\right)$, $\overline{B}_0(x_1, x_2, x_3), \overline{B}_1(x_1, x_2, x_3) \in C^2\left(\mathbb{R}^3\right)$ be given. We seek to determine the vector function $\overline{B}(\overline{x}, t) \in C^2\left(\mathbb{R}^3 \times [0, T]\right)$, which satisfies the following differential equation:

$$\begin{gathered}\frac{\partial^2 \overline{B}}{\partial t^2} = a^2 \Delta \overline{B} + \overline{f}(\overline{x}, t),\ 0 < t < +\infty,\ -\infty < x_1 < +\infty,\ -\infty < x_2 < +\infty,\ 0 < x_3 < +\infty, \\ \overline{B}(x_1, x_2, 0, t) = 0, \\ \overline{B}(x_1, x_2, x_3, 0) = \overline{B}_0(x_1, x_2, x_3), \\ \overline{B}_t(x_1, x_2, x_3, 0) = \overline{B}_1(x_1, x_2, x_3).\end{gathered} \tag{2}$$

The following integral representation for the vector function $\overline{B}(\overline{x}, t)$ is known [9]:

$$\begin{gathered}\overline{B}(\overline{x}, t) = \frac{1}{4\pi a} \frac{\partial}{\partial t} \iint\limits_{S_x^{at}} \frac{\overline{B}_0(\overline{\xi})}{at} d\sigma + \frac{1}{4\pi a} \iint\limits_{S_x^{at}} \frac{\overline{B}_1(\overline{\xi})}{at} d\sigma + \frac{1}{4\pi a^2} \int\limits_0^{at} \left(\iint\limits_{S_M^r} \frac{\overline{f}\left(P, t - \frac{r}{a}\right)}{r} d\sigma \right) dr \\ r = \left|\overline{x} - \overline{\xi}\right| = ((x_1 - \xi_1)^2 + (x_2 - \xi_2)^2 + (x_3 - \xi_3)^2)^{1/2}, P : \overline{\xi} = (\xi_1, \xi_2, \xi_3), \\ M : \overline{x} = (x_1, x_2, x_3).\end{gathered} \tag{3}$$

Expression (3) is obtained by an odd extension of the fundamental solution of the wave equation from the entire space onto the lower half-space (see [24]).

In (3), S_x^{at} denotes a sphere of radius at centered at a point M, which is defined by radius vector $\overline{x}$, and the integration above is performed with respect to coordinates of a point P. In the general case, the Dirichlet boundary condition on the Earth's surface can be inhomogeneous:

$$\overline{B}(x_1, x_2, 0, t) = \overline{\Psi}(x_1, x_2, t) \tag{4}$$

Boundary conditions of the second and third kind are also admissible; however, as shown in [24], an inhomogeneous boundary value problem can be transformed into the boundary setting (3). Therefore, we assume that the field has zero values on the boundary.

As is well known, wave equation solutions in three-dimensional space are determined by initial values specified within a domain called the "cone of dependence" [24]. Observation points can be located in an arbitrary domain of three-dimensional space. Let us assume that all sensors are positioned in the upper half-space. For each observation point $M(\overline{x}, t)$, the cone of dependence K_x^{at} is defined as follows:

$$K_x^{at} = \left\{\overline{\xi} = (\xi_1, \xi_2, \xi_3), \tau : \left|\overline{x} - \overline{\xi}\right| < a(t - \tau)\right\} \tag{5}$$

The vertex of this cone coincides with the point $M(\overline{x}, t)$. The lower base of this cone is denoted by $D_x^{at} = \left\{\overline{\xi} = (\xi_1, \xi_2, \xi_3) : \left|\overline{x} - \overline{\xi}\right| \le at\right\}$. Thus, perturbation at the point $M(\overline{x}, t)$ is non-zero, provided that the initial perturbation intersects D_x^{at} and the wave sources are located within the lateral surface of the cone of dependence K_x^{at}.

The integral representation (3), commonly known as Kirchhoff's formula, allows for the implementation of the local version of the linear integral representation method [17,18], where the Earth is modeled as the lower half-space and the magnetic induction elements are specified in the upper half-space.

Consider formula (2) and a formulation in which an objective functional is minimized, given that the field elements are known in the upper half-space of three-dimensional space. Variational settings within the framework of the linear integral representation method imply that target functions possess some smoothness properties, i.e., they belong to the space $C^2\left(\mathbb{R}^3 \times [0, T]\right)$: $\overline{B}(\overline{x}, t) \in C^2\left(\mathbb{R}^3 \times [0, T]\right)$. Minimization is performed in the norm of $L_2(M_r)$, where $L_2(M_r)$ is the Hilbert space of square-integrable functions defined on domains M_r, $r = 1, \ldots, R$. These domains may be manifolds of various dimensions, such as spatial regions, surfaces, or curves. It should be emphasized that, in most cases, no a priori information regarding the location or geometry of the sources is available. Consequently, all interpretation problems in geophysics must be regularized, as they are inherently ill-posed.

Earlier [17,18], we set variational problems given a fixed set of domains M_r, r = 1, . . . , R. In the present paper, we assume that the unknown source density $\overline{f}(\overline{x},t)$ is to be determined in the entire space. Furthermore, we must emphasize that in spaces with an odd number of dimensions, the so-called "trailing edge" (or "back front") of a wave is observed. This implies that a perturbation may vanish by the time of observation if the field sources do not lie within the cone of dependence of the point $M(\overline{x},t)$.

We propose the following variational setting to determine the unknown source power. Find a function $\overline{f}_*(\overline{x},t) \in C^2\left(\mathbb{R}^3 \times [0,T]\right)$ that satisfies the following conditions:

$$\begin{gathered}
\Omega\left[\overline{f}_*\right] = \min_{\overline{f}(\overline{\xi},t)} \Omega\left[\overline{f}\right], \\
\Omega\left[\overline{f}\right] = \int_0^T d\tau \int_{-\infty}^{+\infty} d\xi_3 \int_{-\infty}^{+\infty} d\xi_2 \int_{-\infty}^{+\infty} d\xi_1 \overline{f}^2(\overline{\xi},\tau)\,, \\
\overline{B}(\overline{x}_i,t_i) = \frac{1}{4\pi a^2} \int_0^{at} \left(\iint\limits_{S_{M_i}^{r_i}} \frac{\overline{f}\left(P, t_i - \frac{r_i}{a}\right)}{r_i} d\sigma \right) dr + \frac{1}{4\pi a^2} \int\limits_{D_{M_i}^{at_i}} \frac{\overline{f}\left(P, t_i - \frac{r_i}{a}\right)}{r_i} d\overline{\xi}, \\
\overline{r}_i = |\overline{x}_i - \xi| = ((x_1^{(i)} - \xi_1)^2 + (x_2^{(i)} - \xi_2)^2 + (x_3^{(i)} - \xi_3)^2)^{1/2}, \overline{\xi} = (\xi_1, \xi_2, \xi_3), \\
\overline{x}_i = \left(x_1^{(i)}, x_2^{(i)}, x_3^{(i)}\right),\ i = 1, \ldots, N.
\end{gathered} \tag{6}$$

The constrained variational problem (6) can be treated as a constrained optimization problem and solved using the method of Lagrange multipliers within the framework of the approximation approach [17]. This transforms (6) into an unconstrained variational problem. Specifically, instead of minimizing the functional $\Omega\left[\overline{f}\right]$ subject to the integral constraints (6) for the magnetic induction components, we minimize an augmented functional $\Phi\left[\overline{f}\right]$. This new functional is defined as the sum of $\Omega\left[\overline{f}\right]$ and the residuals of Equation (6) multiplied by Lagrange multipliers.

Theorem 1. *Suppose the integral representation*

$$\overline{B}(\overline{x}_i,t_i) = \frac{1}{4\pi a^2} \int_0^{at} \left(\iint\limits_{S_{M_i}^{r_i}} \frac{\overline{f}\left(P, t_i - \frac{r_i}{a}\right)}{r_i} d\sigma \right) dr = \frac{1}{4\pi a^2} \int\limits_{D_{M_i}^{at_i}} \frac{\overline{f}\left(P, t_i - \frac{r_i}{a}\right)}{r_i} d\overline{\xi} \tag{7}$$

holds for the vector function $\overline{B}(\overline{x}_i,t_i)$, $\overline{B}(\overline{x},t)$, $\overline{f}(\overline{x},t) \in C^2\left(\mathbb{R}^3 \times [0,T]\right)$. *Here, a is a known parameter representing the wave propagation velocity,* $D_x^{at} = \left\{\overline{\xi} = (\xi_1,\xi_2,\xi_3) : |\overline{x} - \overline{\xi}| \le at\right\}$, $S_x^{at} = \left\{\overline{\xi} = (\xi_1,\xi_2,\xi_3) : |\overline{x} - \overline{\xi}| = at\right\}$.

Then, the function $\overline{f}_*(\overline{x},t) \in C^2\left(\mathbb{R}^3 \times [0,T]\right)$ *is such that*

$$\Phi\left[\overline{f}_*\right] = \min_{\overline{f}(\overline{\xi}.t)} \left\{ \Omega\left[\overline{f}\right] + 2 \sum_{k=1}^{3} \sum_{i=1}^{N} \overline{\lambda}_i^{(k)} \left[B_k(\overline{x}_i,t_i) - \frac{1}{4\pi a^2} \int\limits_{D_{M_i}^{at_i}} \frac{\overline{f}\left(P, t_i - \frac{r_i}{a}\right)}{r_i} d\overline{\xi} \right] \right\}, \tag{8}$$

has the following form:

$$\begin{gathered}
\overline{f}(\boldsymbol{\xi},\tau) = \sum_{j=1}^{N} \frac{\overline{\lambda}_j \theta\left(D_{\mathbf{x}_j}^{at_j}\right)}{|\overline{x}_j - \overline{\xi}|}, \\
|\overline{x}_j - \overline{\xi}| = ((x_1^{(j)} - \xi_1)^2 + (x_2^{(j)} - \xi_2)^2 + (x_3^{(j)} - \xi_3)^2)^{1/2}, \overline{\xi} = (\xi_1, \xi_2, \xi_3), \\
\overline{x}_j = \left(x_1^{(j)}, x_2^{(j)}, x_3^{(j)}\right).
\end{gathered} \tag{9}$$

Proof of Theorem 1. To find the extremum of the objective Function (8) we should compute the functional derivative of (8) with respect to the unknown function $\overline{f}(\overline{x},t)$ and set this derivative to zero:

$$\Phi'\left[\overline{f}_*(\overline{x},t)\right]=0. \tag{10}$$

Expression (10) represents the Euler–Lagrange equation for the variational setting (8), the solution of which is given by (9). (Here we must emphasize that condition (10) is a necessary condition for the extremum of the functional, but not a sufficient condition for its minimum). Therefore, if a minimum of the cost function exists, relation (10) is necessarily satisfied.

In (9), $\theta\left(D_{\mathbf{x}_j}^{at_j}\right)$ is the smoothed (belonging to the space of infinitely differentiable functions) characteristic function of the base $D_{\mathbf{x}_j}^{at_j}$ of the cone of dependence $K_{\mathbf{x}_j}^{at_j}$ with vertex $\overline{x}_i$; $\overline{\Delta}=\left(\overline{\lambda}_1,\overline{\lambda}_2,\ldots,\overline{\lambda}_N\right)^T$, $\overline{\lambda}_j=\left(\lambda_j^{(1)},\lambda_j^{(2)},\lambda_j^{(3)}\right)^T$, is the vector of Lagrange multipliers. Thus, the source density at a given spatial point $\overline{\xi}$ and time τ depends only on those observation points whose cones of dependence contain the given point within their interior. To determine the Lagrange multipliers, we derive the following linear algebraic equations system (LAES):

$$A\overline{\Delta}=\overline{B}_\delta, \tag{11}$$

In (11), $\overline{B}_\delta$ denotes the $3N$-vector of field element values at the observation points (assuming that all three components of the vector field $\overline{B}_\delta$ are known). Alternatively, we can consider only a single field element, such as the z-component. In this case, the dimension of the LAES matrix (11) will be three times smaller (N instead of $3N$). In system (11), matrix A is an $(N\times N)$ matrix with the following property:

$$A=A^T\geq 0. \tag{12}$$

and the elements

$$a_{ij}=\frac{1}{16\pi^2a^4}\int\limits_{D_{M_i}^{at_i}\cap D_{Mj}^{at_j}}\frac{1}{r_ir_j}d\xi \tag{13}$$

It should be emphasized that the matrix elements given by Formula (13) differ significantly from one another. Their expressions depend on whether the centers of the two cones of dependence corresponding to points i and j lie within the intersection of their bases. These matrix elements are computed in accordance with the fundamental principles of the linear integral representations method [16,17] and have the following form:

$$a_{ij}=\begin{cases}4\pi\min\left(R_i,R_j\right)-2\pi R,\ R<R_i,R<R_j,D_{R_i}\cap D_{R_j}=D_{\min(R_i,R_j)},\ O_{\max(R_i,R_j)}\in D_{\min(R_i,R_j)};\\ 2\pi\frac{\left[\min\left(R_i,R_j\right)\right]^2}{R},R<R_i,R>R_j,D_{R_i}\cap D_{R_j}=D_{\min(R_i,R_j)},\ O_{\max(R_i,R_j)}\notin D_{\min(R_i,R_j)};\\ \frac{\pi}{\left|\overline{x}_i-\overline{x}_j\right|}\left\{R_i+R_j-R\right\}^2,R>R_i,R>R_j,R<R_i+R_j;\\ \frac{\pi}{R}\left\{-3R^2+2R_iR+2R_jR+2R_iR_j-R_i^2-R_j^2\right\},\\ R<R_i,R<R_j,D_{R_i}\cap D_{R_j}\neq D_{R_i},D_{R_j},O_{\max(R_i,R_j)}\in D_{\min(R_i,R_j)};\\ \frac{\pi}{R}\left\{-(\max(R_i,R_j)-R)^2+\min(R_i,R_j)(\min(R_i,R_j)+2(\max(R_i,R_j)-R))\right\},\\ R<R_i,R>R_j,D_{R_i}\cap D_{R_j}\neq D_{R_i},D_{R_j},O_{\max(R_i,R_j)}\notin D_{\min(R_i,R_j)},\\ 0,D_{R_i}\cap D_{R_j}=\varnothing.\end{cases}, \tag{14}$$

$R_i=at_i,R_j=at_j,R=\left|\overline{x}_i-\overline{x}_j\right|$.

Formula (14) was obtained analytically by integrating the product of two inverse distances $\left|\overline{x}_j - \overline{\xi}\right|^{-1}$ and $\left|\overline{x}_j - \overline{\xi}\right|^{-1}$ over the intersection of two bases $D_{R_i} \cap D_{R_j}$. This product is symmetric with respect to indices i and j. Therefore, the matrix of LAES (11) is symmetric.

Here, D_{R_i}, D_{R_j} denote two bases of two cones with vertices at points M_i, M_j and radii R_i, R_j, respectively. The centers of these bases (which are balls in three-dimensional space) are denoted by O_{R_i}, O_{R_j}. We assume that the z-axis coincides with the line connecting O_{R_i} and O_{R_j}. The intersection of two bases of the dependence cones is a 3D domain that can be parametrized by spherical coordinates r, ϑ, φ. Since the intersection is axially symmetric, no dependence on φ is observed. The origin of the coordinate system is placed at M_i. In this case, integrating with respect to angle φ will give us 2π. Let us express the distance between the point over the coordinates of which the integration is fulfilled and M_j. We will have

$$R_j = \sqrt{R_i^2 - 2RR_i^2 \cos\ \theta + R^2}.$$

Here, ϑ is the angle in the corresponding spherical system frame.

The expression for the matrix element depends on the location of the centers of the balls and whether they belong to the intersection of the balls or not. Integration with respect to ϑ (this expression looks like $\int_0^{\vartheta^*} \frac{1}{\sqrt{R^2 + r^2 - 2Rr\cos\ \vartheta}} \sin\ \vartheta d\theta$) yields an expression of the form $R_j - R + r$ or $r - R_j + R$, followed by integration with respect to the radius r. The limits of integration with respect to the angle ϑ and the radius depend on the relative positioning of the balls, which serve as the bases of the dependency cones (cones of dependence) for the two observation points under consideration. Finally, we fulfill integrating with respect to r. The diagonal elements of the SLAE matrix will always take the form:

$$a_{ii} = 4\pi R_i, R_i = at_i. \tag{15}$$

□

It should be emphasized that the integration in (6)–(8) is performed over spatial variables. The time dependence is "hidden" within the second argument of the function $\overline{f}\left(P, t_i - \frac{r_i}{a}\right)$ (more precisely, the fourth argument, as this vector function depends on three spatial coordinates and time).

Unlike the stationary version of the S-approximation method, in the case of the wave equation, the elements of the SLAE matrix to which the variational setting (8) is reduced depend significantly on the geometry of the observation network. Consequently, these elements cannot be determined uniformly. This fact must be taken into account when describing periodic processes. In our view, if the observation points are arranged as shown in the third line of (14), the diagonal elements of the matrix will dominate, eliminating the need for a regularization procedure to solve the SLAE (11). Thus, we obtain a well-posed setting for determining the components of a non-stationary vector field.

The integral representation (13) for the matrix elements possesses features of a double-layer potential: integration is performed over the intersection of two balls centered at points M_i and M_j. Here, r_i and r_j denote the distances from points M_i and M_j to the integration point P. As it is well known, a double-layer potential is a discontinuous function when crossing the boundary.

To construct an analytical model of the field element's derivative with respect to the spatial coordinate, one can directly differentiate the integral representations (3) or (7). For

instance, consider representation (6), where the initial field values and their time derivatives are zero. Differentiating expression (7) with respect to x_3 yields

$$\frac{\partial \overline{B}(\overline{x}_i, t_i)}{\partial x_3^{(i)}} = \frac{1}{4\pi a^2} \int\limits_{D_M^{at}} \frac{\overline{f}_{x_3}\left(P, t - \frac{r}{a}\right)}{r} d\overline{\xi}. \tag{16}$$

This expression is obtained by shifting from the global coordinate system to a local one centered at point M_i, performing the differentiation, and then returning to the initial frame.

Equation (16) employs the so-called "retarded potential" (or "time-delayed potential"). Since a wave propagates at a finite velocity a, the perturbation at the observation point depends on the source density evaluated at an earlier moment, $t - \frac{r}{a}$.

When seeking analytical approximations for the functions $\overline{B}_0(\overline{\xi}), \overline{B}_1(\overline{\xi}), \overline{f}\left(P, t - \frac{r}{a}\right)$, the primary computational challenge is to determine stable solutions for the LAES that correlate with the a priori information. Here, $r = \left|\overline{x} - \overline{\xi}\right|$.

Note 1. We initially considered the variational setting (8) in a spherical domain. A more rigorous formulation is as follows:

Determine: $\widetilde{f}_*(\overline{x}) \in C^2\left(\mathbb{R}^3\right)$ such that:

$$\Phi\left[\overline{f}_*\right] = \min_{\overline{f}(\overline{\xi}, t)} \left\{ \widetilde{\Omega}\left[\overline{f}\right] + 2 \sum_{k=1}^{3} \sum_{i=1}^{N} \lambda_i^{(k)} \left[\overline{B}(\overline{x}_i, t_i) - \frac{1}{4\pi a^2} \int\limits_{D_{M_i}^{at_i}} \frac{\overline{f}(P)}{r_i} d\overline{\xi} \right] \right\} \tag{17}$$

is satisfied. Here,

$$\widetilde{\Omega}\left[\overline{f}\right] = \int\limits_{-\infty}^{+\infty} d\xi_3 \int\limits_{-\infty}^{+\infty} d\xi_2 \int\limits_{-\infty}^{+\infty} d\xi_1 \overline{f}^2(\overline{\xi}) \tag{18}$$

Function $\overline{f}_*(\overline{x})$ has the following form:

$$\begin{gathered} \overline{f}(\overline{\xi}, \tau) = \sum_{j=1}^{N} \frac{\overline{\lambda}_j \theta\left(\Gamma K_{x_j}^{at_j}\right)}{\left|\overline{x}_j - \overline{\xi}\right|}, \\ r_j = \left|\overline{x}_j - \overline{\xi}\right| = ((x_1^{(j)} - \xi_1)^2 + (x_2^{(j)} - \xi_2)^2 + (x_3^{(j)} - \xi_3)^2)^{1/2}, \overline{\xi} = (\xi_1, \xi_2, \xi_3), \\ \overline{x}_j = \left(x_1^{(j)}, x_2^{(j)}, x_3^{(j)}\right). \end{gathered} \tag{19}$$

$\theta\left(\Gamma K_{\mathbf{x}_j}^{at_j}\right)$ is in (19) the smoothed characteristic function of the lateral surface of the cone of dependence for point $\overline{x}_j$. The Lagrange multipliers $\overline{\lambda}_j, j = 1, 2, \ldots, N$, are found by solving an LAES similar to (11) whose matrix elements (20) can be expressed via elementary functions:

$$\begin{gathered} a_{ij} = \frac{1}{16\pi^2 a^4} \int\limits_{\Gamma K_{M_i}^{at_i} \cap \Gamma K_{Mj}^{at_j}} \frac{1}{r_i r_j} d\overline{\xi} = \frac{b}{8\pi a^4} \int\limits_{\cos\vartheta^* + \alpha}^{1+\alpha} \frac{\sqrt{d^2 - z^2} dz}{z(z + 2\alpha)}, \\ b = \frac{R_{ij}^2 - (\Delta R)^2}{2R_{ij}}, d = \sqrt{2 + \alpha^2}, \cos\vartheta^* = \frac{R_i^2 + R_{ij}^2 - R_j^2}{2R_i R_{ij}}, \alpha = \frac{R_i - R_j}{R_{ij}}. \end{gathered} \tag{20}$$

In (20), $R_{ij} = \left|\overline{x}_i - \overline{x}_j\right|$. However, we recommend computing these integrals numerically, as the analytical formulas are excessively long.

Two methods from our previous studies [27] were implemented to solve system (11): the block Cholesky regularization method (BCM) and the refined block method (RBM). Both are based on an adaptive filtering algorithm. In the first stage, the LAES is solved using the entire dataset. In the second stage, certain matrix blocks are excluded if they

do not significantly affect the relative accuracy. Regularization parameters are selected individually for each block.

If the observation points are far apart, the diagonal elements dominate. Furthermore, the cones of dependence for adjacent points may not intersect at all, resulting in zero-valued matrix elements. Conversely, if observation points are too close, the LAES matrix becomes ill-conditioned, as the elements differ very little. Thus, this method allows for both the determination of spatio-temporal field distributions and the analysis of input data quality, including the configuration of the observation network. If the matrix element is significantly smaller than the diagonal elements, it is not recommended to include those observation points in the approximation.

3. Results

A new method for constructing a mathematical model of gravity field variations from Satellite Mission GRACE data [22] was tested. The study focused on a region near Volcano Kanlaon, Philippines, considering a uniform observation network. Figure 1 displays the map of gravity field variations, and Figure 2 presents the map of the differences between approximated and measured field values, including 6000 points in one case and 10,000 gravity field values in another.

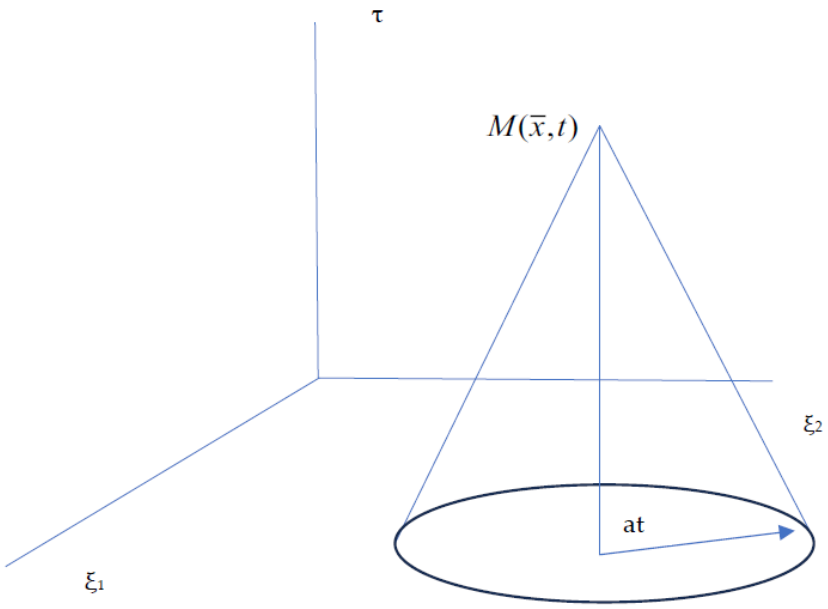


Figure 1. Cone of dependence K_x^{at} of point $M(\overline{x}, t)$.

Initially, S-approximations of the gravity field were constructed using two methods: BCM and RBM [27]. Sensors (observation points) were positioned at an altitude of 500 km. Subsequently, a "non-stationary" gravity field model was developed. We analyzed data obtained over 10 months, employing two values for the parameter a^2 (100 and 1000). We considered the gravity field values at a point, measured at a virtual moment of time $\overline{x}_i$:

$$t_i = \frac{g(\overline{x}_i)}{a},\ g(\overline{x}_i) = \alpha h + 0.12\gamma_i, h = \sqrt[3]{h_1 h_2 h_3}. \tag{21}$$

These values were designated as $\overline{B}(\overline{x}_i, t_i)$. In Equation (21), $h_p, p = 1, 2, 3$, represents steps with respect to the direction x_p. In our case, the steps with respect to directions x_1, x_2 were set to 2 km, while the step with respect to the direction x_3 was 10 km. γ_i denotes a random variable uniformly distributed on the interval $[-1, 1]$. Time can be incorporated

into our model when dealing with a stationary field element or when the time dependence law is unknown.

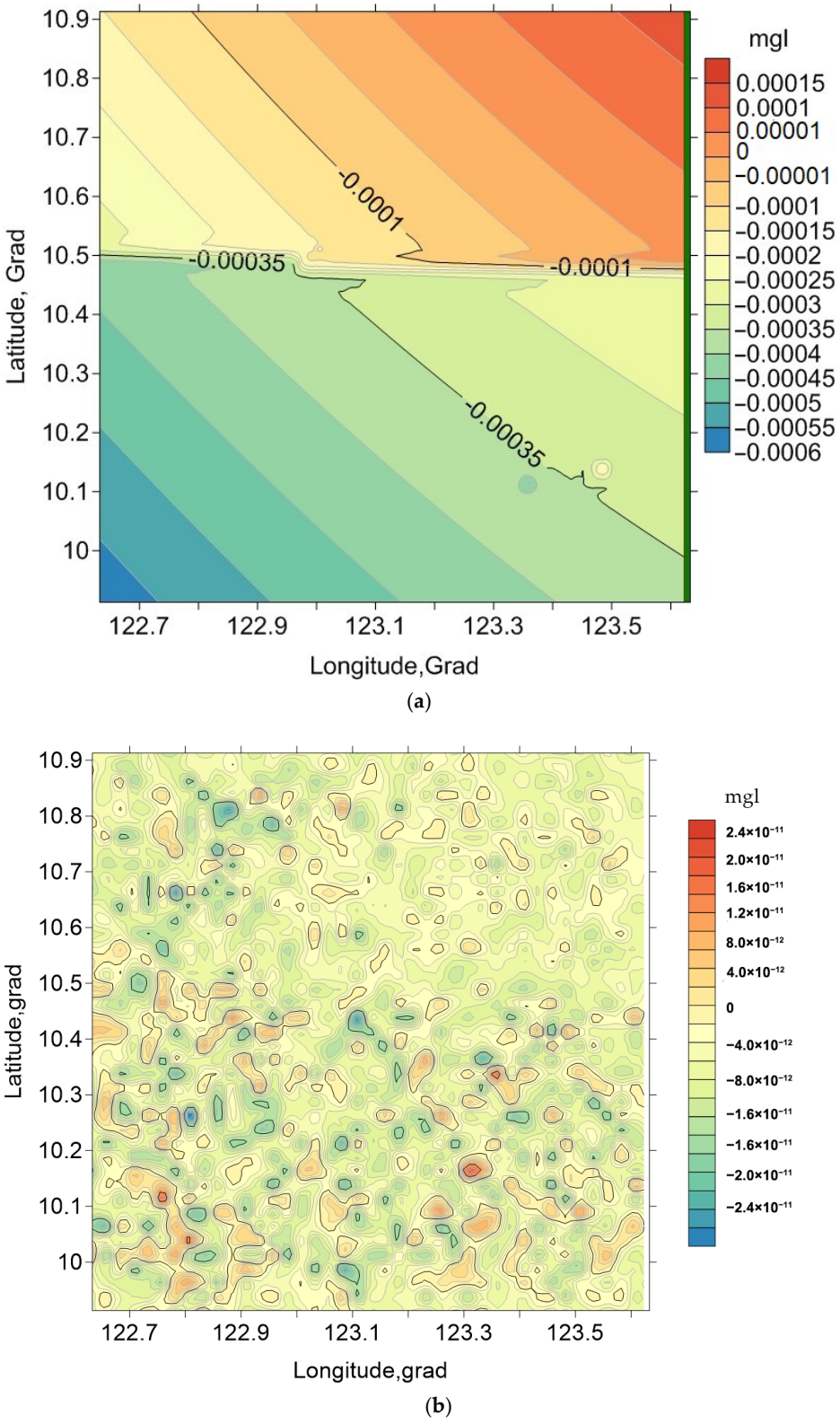


Figure 2. (**a**) Gravity field variations near Volcano Kanlaon according to the GRACE DATA. (**b**) Difference map of the approximated Gravity Field.

Parameter α was introduced in order to reveal the most important features of the network geometry. This parameter varied from 0.001 to 10. The small values of this

parameter correspond to the matrix elements (14) given in the last line. It means that the cones of dependence for two adjacent points do not intersect. In this case, we have a well-posed problem that has a unique solution.

If α approaches 0.6, then we can use the third expression from (14) for the matrix elements. The SLAE matrix is non-singular. Since the matrix of the system of linear equations is non-singular, the inverse problem can be considered well-posed [28]. Equation (14) indicates that the hypothetical moments of time in the dataset differed from each other by a maximum of 20 percent.

Large (greater than 1) values of α correspond to either the first line of (14) or the fourth and fifth lines of this formula. This fact can be clarified as follows. The bases of the cones of dependence have a non-empty intersection if the moments in time t_i and t_j are both sufficiently large, or if one of the two points M_i and M_j lies within the cone of dependence corresponding to the other point. In this case, we encounter a badly conditioned linear algebraic equation system (SLAE).

If real-time-dependent physical field values are provided, the integral representation (7) can be directly applied. In this scenario, the moments in time will not be correlated with spatial coordinates. However, for satellite observations, the moments in time and sensor coordinates are linked due to the satellite's movement along a defined trajectory.

We derived a function $\mathbf{f}\left(P, t - \frac{r}{a}\right)$ from the variational problem (6), which, as previously emphasized, reduces to solving a system of linear algebraic equations (SLAE). Sensors were selected from the real dataset and from a set generated by modified S-approximations, ensuring that the matrix elements are as follows:

$$\frac{\pi}{\left|\overline{x}_i - \overline{x}_j\right|}\left\{R_i + R_j - R\right\}^2, R > R_i, R > R_j, R < R_i + R_j \tag{22}$$

Therefore, we can conclude that the joint implementation of various versions of the S-approximation method (i.e., stationary and non-stationary versions of the linear integral representation method) expands research horizons and enhances the quality of the obtained approximate solution to a variational problem.

The approximation quality index $\Delta = \frac{\|Ax - f_\delta\|_E}{\|f_\delta\|_E}$ in the stationary case was:

- $2.1 \cdot 10^{-9}$ for the set of 10,000 points.
- $4.1 \cdot 10^{-8}$ for the set containing 16,000 points.

Here, x is the vector of Lagrange multipliers from system (9), and f_δ is the vector on the right-hand side, including noise of varying intensity. $\|f_\delta\|_E$ denotes the Euclidean norm of a vector.

The root mean square error $\sigma = \frac{\|Ax - f_\delta\|_E}{\sqrt{N}}$, the upper error estimate $\sigma_{\max} = \sqrt{\frac{\delta^2_{\max}}{N}}$, and the lower error estimate $\sigma_{\min} = \sqrt{\frac{\delta^2_{\min}}{N}}$ in the stationary case were:

- For the set of 16,000 points: $\sigma_{\max}$ = 0.0002 μGal, $\sigma_{\min}$ = 0.00015 μGal.
- For the set of 10,000 points: $\sigma_{\max}$ = 0.00015 μGal; $\sigma_{\min}$ = 0.0001 μGal.

Non-stationary approximations were also constructed for two sets containing the same number of field elements (though with different values compared to the stationary case). The quality index for the set of 16,000 points was:

Δ = 0.00003, $\alpha = 0.7$,
Δ = 0.000015, $\alpha = 0.5$,
Δ = 0.0000015, $\alpha = 0.2$,
$\Delta = 1.2 \cdot 10^{-8} \div 1 \cdot 10^{-6}$, $\alpha = 0.001 \div 0.1$.
and for the set of 10,000 points, it was:
Δ = 0.00002, $\alpha = 0.7$,

$\Delta = 0.00001$, $\alpha = 0.5$,
$\Delta = 0.000001$, $\alpha = 0.2$,
$\Delta = 6.4 \cdot 10^{-9} \div 3 \cdot 10^{-7}$, $\alpha = 0.001 \div 0.1$.

We cannot obtain a stable approximate solution to LAES (11) in the case of large values of the parameter α (if this entity is greater than 2). We can state that the corresponding ill-posed problem can not be regularized.

We also conducted a series of mathematical experiments to test the sensitivity of the method to errors in the right-hand side of the system of linear algebraic Equation (11). A detailed description of how errors in the right-hand side affect the results of solving inverse geophysical problems can be found, for example, in the work of V.N. Strakhov [29]. For this purpose, we perturbed the right-hand side (GRACE data) by adding a random variable uniformly distributed on the interval $[-1, 1]$, such that the ratio of the Euclidean norms of the noise vector and the useful signal $\varepsilon = \frac{\|\delta f\|_E}{\|f_\delta\|_E}$ was $10^{-7}, 10^{-6}, 10^{-4}, 10^{-2}$.

We then solved system (11) for the set of 10,000 points using two methods previously proposed by us [27], as well as the SVD method (singular value decomposition [30]), parameter α being set to 0.2. When using BCM and RBM, the quality index Δ was:

$$1.3 \cdot 10^{-5}, \varepsilon = 10^{-7},$$
$$2.5 \cdot 10^{-4}, \varepsilon = 10^{-6},$$
$$3.1 \cdot 10^{-3}, \varepsilon = 10^{-4},$$
$$4.8 \cdot 10^{-1}, \varepsilon = 10^{-2}.$$

SVD method gave the following results for Δ:

$$2.6 \cdot 10^{-4}, \varepsilon = 10^{-7},$$
$$1.5 \cdot 10^{-3}, \varepsilon = 10^{-6},$$
$$1.1 \cdot 10^{-2}, \varepsilon = 10^{-4},$$
$$7.2 \cdot 10^{-1}, \varepsilon = 10^{-2}.$$

We can see that the regularized Cholesky method and the regularized block method elaborated within the S-approximation technique are more effective than the SVD method. The superior convergence can be explained by the flexible and customizable regularization procedure incorporated into our method. Numerous studies have addressed the convergence criteria for various algorithms used to solve inverse problems (see, e.g., [31,32]), as this aspect is of fundamental importance when selecting a particular method for solving interpretation-oriented tasks.

Future research will concentrate on developing stable algorithms for computing linear transforms of non-stationary fields, such as finding higher derivatives of the gravity potential and performing downward analytical continuation of fields towards their sources. Additionally, we plan to identify the conditions for the unique solvability of system (9). This is crucial for yielding stable approximate solutions to the variational problem (9). If the matrix of the SLAE is ill-conditioned, then a unique solution does not exist. However, regularization of the variational problem can be accomplished in such cases, enabling a robust interpretation of the variational field data.

4. Discussion

This paper proposes a novel version of the linear integral representation method applicable not only for the interpretation of data related to non-stationary geophysical fields but also for the qualitative and quantitative analysis of observation network characteristics. We applied the linear integral representation method to solve the inverse problem of determining a three-dimensional continuously distributed wave source. It was assumed that

the measured signal satisfies a wave equation with constant coefficients and homogeneous initial-boundary conditions. Notably, the vector function describing the source, which generally depends on an infinite number of parameters, was reconstructed from finite and approximate field data. Furthermore, the observation network used to define the field elements was not restricted to a regular grid and could be arbitrary.

This analysis helps in defining objectives for further research within the studied region. The new technique for solving linear inverse problems in geophysics encompasses: (1) establishing a variational problem, (2) defining the domain of dependence for each observation point, (3) selecting the most efficient algorithm for determining a stable approximate solution to the posed problem, and (4) formulating recommendations for improving interpretation quality.

The variational formulation for finding the minimum-norm solution to the inverse problem reduces to a system of linear algebraic equations (LAES) with an approximately given right-hand side. The matrix of this system possesses specific properties: when applying a variant of the variational approach proposed by V.N. Strakhov [17], the matrix is symmetric positive semidefinite. However, the primary difficulty in solving such systems lies in the fact that the minimum eigenvalue of the matrix may be close to zero. In this case, the system becomes ill-conditioned and requires regularization using established methods [33–39]. We have previously proposed several regularizing algorithms for solving large-scale and ultra-large-scale ill-conditioned systems. The algorithms we have developed for solving large and ultra-large systems of linear algebraic equations—to which virtually all geophysically meaningful inverse problems are reduced—make it possible to find linear field transforms and analytic continuations of geophysical fields toward the sources. Furthermore, they allow for estimating the thickness and geometry of anomalous field sources even in cases where information about the anomalous fields of the Earth and planets is incomplete, heterogeneous, and of varying accuracy [40,41].

In implementing the non-stationary version of the S-approximation, a critical aspect is the investigation of the observation network and the replenishment of the database using provided tools, such as the stationary S-approximation. Matrix properties are most distinctly revealed in the non-stationary version of the linear integral representation method: when observation points are located far apart, the corresponding matrix elements become zero. Conversely, in the stationary case, this does not hold, and an SLAE cannot be effectively regularized, particularly when analyzing so-called profile data. The method allows for the determination of values of certain linear functionals from the values of other linear functionals. In geophysical practice, this means that from known values of a field element at points within an observation network, one can determine linear transforms of the corresponding field. These transforms include higher derivatives of gravitational or magnetic potentials and downward analytical continuations of the field towards its sources. Crucially, this does not require the introduction of "artificial" approximation constructs. Instead, the observation network points (their geometry and relative positions) largely dictate the quality of the constructed analytical model of the investigated geophysical field.

5. Conclusions

A new method for the mathematical modeling of non-stationary physical fields based on linear integral representations is proposed. The sources of these non-stationary fields can be determined from the solutions of linear algebraic equation systems with a non-negative symmetric matrix. Our main result is the analytical derivation of expressions for the matrix elements of the system of linear algebraic equations (LAES) to which the linear inverse problem of finding an unknown wave source is reduced. Having an analytical expression for the matrix elements is of fundamental importance in such studies, as this

approach avoids introducing additional errors into the input data. The forward problem operator remains exact and does not require approximation through the discretization of differential or integral equations. These expressions were obtained by analyzing the symmetry of the intersection area of the dependence cones for each pair of observation points. Given the variational formulation described in this paper, the resulting matrix elements are particularly simple and can be expressed in terms of elementary functions, as previously demonstrated in our development of the S-approximation method.

It is important to note that in the general case, field sources depend on an infinite number of parameters. We have developed an algorithm that reduces the interpretation problem to solving a finite number of linear algebraic equations, ensuring the stability of the regularized approximate solution. In some instances, matrix elements can be obtained analytically, thereby reducing the ambiguity of the problem statement. We solved the systems of linear algebraic equations arising from the linear integral representation method using both our original, previously developed techniques and the widely known SVD method. Our regularized Cholesky decomposition and regularized block method achieved an approximation quality for the non-stationary field element approximately an order of magnitude better. This is likely due to the greater flexibility of regularized solvers compared to standard direct methods that lack an adaptive regularization mechanism. Such adaptive algorithms essentially "tune" themselves to a specific system to find a solution that is robust to noise in the right-hand side. To test the sensitivity of the methodology, we artificially contaminated the GRACE mission data with a uniformly distributed error on the interval $(-1, 1)$. Our approach yields, in our view, satisfactory results. Future efforts will focus on the analytical representability of matrix elements for variational formulations in spherical, parabolic, and other coordinate systems, as well as on obtaining more rigorous results regarding the uniqueness of the inverse problem solution for the wave operator in three-dimensional space.

Author Contributions: Conceptualization, I.S. and I.K.; methodology, I.S. and A.S.; software, I.S. and A.L.; validation, A.S. and I.K.; formal analysis, I.K.; investigation, I.S. and A.S.; writing—original draft preparation, I.S. and A.S.; writing—review and editing, I.S. and A.L.; visualization, I.S.; supervision, I.S.; project administration, I.S. All authors have read and agreed to the published version of the manuscript.

Funding: This research was funded by the State Assignment of the Institute of Physics of the Earth RAS, theme number FMWU-2025-0030.

Data Availability Statement: The original contributions presented in this study are included in the article. Further inquiries can be directed to the corresponding author.

Conflicts of Interest: The authors declare no conflicts of interest.

Abbreviations

The following abbreviations are used in this manuscript:

$\overline{v}(\overline{r},t)$, $\overline{B}(\overline{r},t)$	velocity field and magnetic induction depending on spatial coordinates $\overline{r}$= (x_1, x_2, x_3) and time t.
S_x^{at}	denotes a sphere of radius at centered at point M, which is defined by radius vector $\overline{x} = (x_1, x_2, x_3)$.
$C^2(\mathbb{R}^3 \times [0,T])$	denotes the space of twice continuously differentiable functions in the direct product $\mathbb{R}^3 \times [0,T]$.
K_x^{at}	denotes the cone of dependence.
$\overline{f}(\overline{x},t)$	denotes the wave source.
$L_2(M_r)$	denotes the space of measurable square-integrable functions.

SLAE	System of Linear Algebraic Equations
BCM	Regularized Block Cholesky Method
RBM	Refined Block Method

References

1. Backus, G.; Gilbert, F. Numerical application of formalism for geophysical inverse problems. *Geophys. J. Roy. Astr. Soc.* **1967**, *13*, 247–276. [CrossRef]
2. Backus, G.; Gilbert, J.F. The resolving power of gross Earth data. *Geophys. J. Roy. Astr. Soc.* **1968**, *16*, 169–205. [CrossRef]
3. Backus, G.; Gilbert, J.F. Uniqueness in the inversion of inaccurate gross Earth data. *Phil. Trans. Roy. Soc. A* **1970**, *266*, 123–192.
4. Cai, C.; Wang, Z.; Xu, J.; Zou, Y. Theoretical Foundation of Finite Frequency Control. In *Finite Frequency Analysis and Synthesis for Singularly Perturbed Systems*; Studies in Systems, Decision and Control; Springer: Cham, Switzerland, 2017; Volume 78. [CrossRef]
5. Christophe, Z. Seismic tomography using parameter-free Backus–Gilbert inversion. *Geophys. J. Int.* **2019**, *21*, 619–630.
6. Del Debbio, L.; Lupo, A.; Panero, M.; Tantalo, N. Bayesian solution to the inverse problem and its relation to Backus–Gilbertmethods. *Eur. Phys. J.* **2025**, *85*, 185. [CrossRef]
7. Hansen MALupo, A.; Tantalo, N. Extraction of spectral densities from lattice correlators. *Phys. Rev. D* **2019**, *99*, 094508. [CrossRef]
8. Yamamoto, M. Stability, reconstruction and regularization for an inverse source hyperbolic problem by a control method. *Inverse Probl.* **1995**, *11*, 481–496. [CrossRef]
9. Yamamoto, M. Determination of forces in vibrations of beams and plates by pointwise and line observations. *J. Inverse Ill-Posed Probl.* **1996**, *4*, 437–457. [CrossRef]
10. Liu, Y.; Yamamoto, M. On the multiple hyperbolic systems modeling phase transformation kinetics. *Appl. Anal.* **2014**, *93*, 1297–1318. [CrossRef]
11. Liu, Y.; Jiang, D.; Yamamoto, M. Inverse source problem for a double hyperbolic equation describing the three-dimensional time cone model. *SIAM J. Appl. Math.* **2015**, *75*, 2610–2635. [CrossRef]
12. Shu, C.; Wu, W.X.; Wang, C.M. Analysis of metallic waveguides by using least square-based finite difference method. *Comput. Mater. Contin.* **2005**, *2*, 189–200.
13. Yamamoto, M. Conditional Stability in Determination of Force Terms of Heat Equations in a Rectangle. *Math. Comput. Model.* **1993**, *18*, 79–88. [CrossRef]
14. Ohe, T.; Inui, H.; Ohnaka, K. Real-time reconstruction of time-varying point sources in a three-dimensional scalar wave equation. *Inverse Probl.* **2011**, *27*, 115011. [CrossRef]
15. Liu, C.S. An integral equation method to recover non-additive and non-separable heat source without initial temperature. *Int. J. Heat Mass Transfer.* **2016**, *97*, 943–953. [CrossRef]
16. Liu, C.S.; Chang, C.W. A global boundary integral equation method for recovering space-time dependent heat source. *Int. J. Heat Mass Transfer.* **2016**, *92*, 1034–1040. [CrossRef]
17. Strakhov, V.; Stepanova, I. Solution of gravity problems by the S-approximation method (Regional Version). *Izv. Phys. Solid Earth* **2002**, *16*, 535–544.
18. Stepanova, I.E.; Kolotov, I.I. Variational Formulations for Wave and Heat Conductivity Equations within the Framework of Discrete Potential Theory. *Doklady. Earth Sci.* **2025**, *522*, 18. [CrossRef]
19. Hood, L.; Oliveira, J.; Galluzzi, V.; Rothery, D. Investigating sources of Mercury's crustal magnetic field: Further mapping of Messenger magnetometer data. *JGR Planets* **2018**, *123*, 2647–2666. [CrossRef]
20. Zhang, Y.; Lukyanenko, D.; Yagola, A. An optimal regularization method for convolution equations on the sourcewise represented set. *J. Inverse ILL-Posed Probl.* **2016**, *23*, 465–475. [CrossRef]
21. Johnson, C.L.; Mittelholz, A.; Langlais, B.; Russell, C.T.; Ansan, V.; Banfield, D.; Chi, P.J.; Fillingim, M.O.; Forget, F.; Haviland, H.F.; et al. Crustal and time-varying magnetic fields at the InSight landing site on Mars. *Nat. Geosci.* **2020**, *13*, 199–204. [CrossRef]
22. Available online: https://grace.jpl.nasa.gov/ (accessed on 3 August 2019).
23. Wang, Y.; Kolotov, I.I.; Lukyanenko, D.V.; Yagola, A.G. Reconstruction of magnetic susceptibility using full magnetic gradient data. *Comput. Math. Math. Phys.* **2020**, *60*, 1000–1007. [CrossRef]
24. Mikhailov, V.P. *Partial Differential Equations*; Mir Publishers: Mir, Moscow, 1978.
25. Kolotov, I.; Lukyanenko, D.; Stepanova, I.; Wang, Y.; Yagola, A. Recovering the near-surface magnetic image of Mercury from satellite observations. *Remote. Sens.* **2023**, *15*, 2125. [CrossRef]
26. Arnold, V.I.; Khesin, B.A. *Topological Methods in Hydrodynamics*; Springer: New York, NY, USA, 2021; 455p.
27. Salnikov, A.; Stepanova, I.; Gudkova, T.; Batov, A. Analytical modeling of the magnetic field of Mars from satellite data using modified S-approximations. *Dokl. Earth Sci.* **2021**, *499*, 575–579. [CrossRef]
28. Seidman, T.I.; Vogel, C.R. Well-posedness and convergence of some regularization methods for non-linear ill-posed problems. *Inverse Probl.* **1989**, *5*, 227–238. [CrossRef]

29. Strakhov, V.N. Processing of geophysical information under multiplicate-additive noise. *Dokl. Akad. Nauk SSSR* **1991**, *319*, 599–603.
30. Golub, G.H. Least square, singular values and matrix approximations. *Appl. Math.* **1968**, *13*, 44–51. [CrossRef]
31. Kindermann, S.; Neubauer, A. On the convergence of the quasi-optimality criterion for (iterated) Tikhonov regularization. *Inverse Probl. Imaging* **2008**, *2*, 291–299. [CrossRef]
32. Yuan, Q.; Zhang, Y. Convergence of a regularization algorithm for nonexpansive and monotone operators in Hilbert spaces. *Fixed Point Theory Appl.* **2014**, *2014*, 180. [CrossRef]
33. Bauer, F.; Reiss, M. Regularization independent of the noise level: An analysis on quasi-optimality. *Inverse Probl.* **2008**, *24*, 055009. [CrossRef]
34. Zhang, Y.; Hofmann, B. Two new non-negativity preserving iterative regularization methods for ill-posed inverse problems. *Inverse Probl. Imaging* **2021**, *15*, 229–256. [CrossRef]
35. Zhang, Y.; Hofmann, B. On the second-order asymptotical regularization of linear ill-posed inverse problems. *Appl. Anal.* **2020**, *99*, 1000–1025. [CrossRef]
36. Zhang, Y.; Gulliksson, M.; Bennetts, V.M.H.; Schaffernicht, E. Reconstructing gas distribution maps via an adaptive sparse regularization algorithm. *Inverse Probl. Sci. Eng.* **2016**, *24*, 1186–1204. [CrossRef]
37. Hancen, P.C. Numerical tools for analysis and solution of Fredholm integral equations of the first kind. *Inverse Probl.* **1992**, *8*, 849–872. [CrossRef]
38. Leonov, A.S. Extra-optimal methods for solving ill-posed problems. *J. Inverse Ill-Posed Probl.* **2012**, *20*, 637–665. [CrossRef]
39. Leonov, A.S.; Wang, Y.; Yagola, A. Piecewise uniform regularization for the inverse problem of the microtomography with a-posteriori estimate. *Inverse Probl. Sci. Eng.* **2020**, *28*, 448–458. [CrossRef]
40. Kim, D.; Banerdt, W.B.; Ceylan, S.; Giardini, D.; Lekić, V.; Lognonné, P.; Beghein, C.; Beucler, É.; Carrasco, S.; Charalambous, C.; et al. Surface waves and crustal structure on Mars. *Science* **2022**, *378*, 417–421. [CrossRef]
41. Stepanova, I.E.; Shchepetilov, A.V.; Mikhailov, P.S. Analytical Models of Time-Dependent Physical Fields of the Earth: Local Version. *Izv. Phys. Solid Earth* **2023**, *59*, 120–134. [CrossRef]

Disclaimer/Publisher's Note: The statements, opinions and data contained in all publications are solely those of the individual author(s) and contributor(s) and not of MDPI and/or the editor(s). MDPI and/or the editor(s) disclaim responsibility for any injury to people or property resulting from any ideas, methods, instructions or products referred to in the content.